Taylor & Francis
Taylor & Francis Group

RESEARCH ARTICLE

🔓 OPEN ACCESS ✓ Check for updates

Emodin in *Rheum undulatum* inhibits oxidative stress in the liver via AMPK with Hippo/Yap signalling pathway

Eun Hye Lee[a]*, Su Youn Baek[b]*, Ji Young Park[a] and Young Woo Kim[c] (iD)

[a]Department of Biomedical Science, Kyungpook National University, Daegu, Korea; [b]Institute for Phylogenomics and Evolution, Kyungpook National University, Daegu, Korea; [c]School of Korean Medicine, Dongguk University, Gyeongju, Korea

ABSTRACT

Context: Emodin is a compound in *Rheum undulatum* Linne (Polygonaceae) that has been reported to exert anti-inflammatory, antibacterial, and antiallergic effects.

Objective: Oxidative stress is a causative agent of liver inflammation that may lead to fibrosis and hepato-carcinoma. In this study, we investigated the antioxidant effects of emodin and its mechanism.

Materials and methods: We used the hepatocyte stimulated by arachidonic acid (AA) + iron cotreatment and the C57B/6 mice orally injected with acetaminophen (APAP, 500 mg/kg, 6 h), as assessed by immunoblot and next generation sequencing (NGS). Emodin was pre-treated in hepatocyte ($3 \sim 30 \mu M$) for 1 h before AA + iron, and in mice (10 and 30 m/kg, P.O.) for 3 days before APAP.

Results: *In vitro*, emodin treatment inhibited the cell death induced by AA + iron maximally at a dose of 10 μM ($EC_{50} > 3 \mu M$). In addition, emodin attenuated the decrease of anti-apoptotic proteins, and restored mitochondria membrane potential as mediated by the liver kinase B1 (LKB1)-AMP-activated protein kinase (AMPK) pathway. LKB1 mediated AMPK activation was verified using the LKB1 deficient cell line, HeLa. Emodin (10 μM; after 10 min) also induced the phosphorylation of Yes-associated protein 1 (YAP1), the main downstream target of the Hippo signalling pathway that mediated oxidative stress or the ROS-initiated signalling pathway. *In vivo*, the oral treatment of emodin (10 and 30 m/kg, 3 days) decreased APAP-induced hepatic damage, as indicated by decreases in antioxidant genes as well as tissue damage.

Conclusion: Our results show that emodin inhibits oxidative liver injury via the AMPK/YAP mediated pathway.

Introduction

Rheum undulatum Linne (Polygonaceae) is a traditional herbal medicine in East Asian countries used for haematemesis, melena, and menorrhagia (Matsuda et al. 2001). The reported pharmacological effects of *R. undunalum* include improving movement of the colon, liver protection, antibacterial, anti-inflammatory, and anti-aging effects. Components of *R. undulatum* include rhein, emodin, aloe-emodin, sennoside A, chrysophanol, and resveratrol (Lee et al. 2003; Yoo et al. 2007). Although emodin is present in several plants including those of the genera *Aloe and Cassia*, *Rheum undulatum* is a representative plant having emodin as an active component in traditional oriental medicine. Emodin has been shown to have various effects (Chen et al. 2002; Xue et al. 2010; Pang et al. 2015). However, its effects on liver damage are not fully understood and its mechanisms have not been clearly investigated.

Oxidative stress, which is a major cause of various liver diseases (Li et al. 2015), is defined as break-down of the physiological balance between reactive oxygen species (ROS) and the body efficacy of ROS removal (Gupta et al. 2014). ROS and inflammatory cytokines promote activation of phospholipases, and phospholipase A_2 (PLA_2) stimulates the release of arachidonic acid (AA) (Gijón et al. 2000; Shin and Kim 2009). Liberated AA serves as a substrate of oxidation by the action of cyclooxygenase (COX) to generate eicsanoids. AA mediates oxidative stress, DNA damage, protein oxidation, inflammatory responses, and cell death (Kim et al. 2009).

Iron is an essential transition metal that maintains oxygen utilization in our bodies. The majority of iron in humans is stored in the liver, spleen and bone marrow (Purohit and Brenner 2006). However, when excess iron exists, it may result in inflammatory conditions and cause higher release of AA, enhancing oxidative stress (Shin and Kim 2009). Therefore, a combination of AA and iron is used as an oxidative stress inducer in many studies because of its synergistic toxicity, in which iron might play a role as a catalyst of oxidation (Caro and Cederbaum 2001; Shin and Kim 2009; Dong et al. 2014; Choi et al. 2016).

Various types of signalling might be involved in the pathological process of oxidative stress in the cells. AMPK is a heterotrimer kinase complex consisting of α, β and γ subunits (Horie et al. 2008) that play a critical role in energy homeostasis by responding to low cellular energy (Emerling et al. 2009).

Co-treatment with AA and iron is known to produce increased oxidative stress, which were successfully inhibited by some beneficial compounds including oltipraz, isorhamnetin, isoliquiritigenin, sauchinone and metformin via AMP-activated protein kinase (AMPK)-related pathway oxidation (Caro and Cederbaum 2001; Shin and Kim 2009; Dong et al. 2014; Choi et al. 2016).

Therefore, we verified the protective effects of emodin against oxidative stress induced by AA + iron in hepatocyte. We found that emodin exerts hepatocyte protective effects against AA + iron induced oxidative stress. Emodin was also applied in acetaminophen (paracetamol, APAP)-induced acute liver damage model, the representative model of oxidative stress *in vivo*. In mice, emodin attenuated hepatocyte damage and the dysregulation of antioxidant enzyme in the tissue sample. Moreover, we found that emodin regulated AMPK and Hippo signalling, which are closely related to oxidative stress (Wada et al. 2011; Xiao et al. 2011, Morinaka et al. 2011), suggesting that these signalling pathways influence the effects of emodin in the liver, as indicated by next generation sequencing (NGS), immunoblot and immunohistochemical analysis.

Materials and methods

Reagents

Emodin, dimethylsulphoxide (DMSO), ferric nitrate, nitrilotriacetic acid, 3-(4,5-dimethylthiazol-2-yl)- 2,5-diphenyl-tetrazolium bromide (MTT), rhodamine 123 (Rh123), 2′,7′-dichlorofluorescein diacetate (DCFH-DA) were purchased from Sigma (St. Louis, MO, USA). Anti-PARP, anti-procaspase-3, anti-Bcl-xL, anti-phospho-acetyl-CoA carboxylase (ACC), anti-AMPKα, anti-phospho-AMPKα, anti-LKB1, anti-phospho-LKB1, anti-Yes-

associated protein (YAP), and anti-phospho-YAP antibodies were obtained from Cell Signalling Technology (Beverly, MA, USA).

Cell culture

HepG2, SK-Hep-1, Huh-7 and HeLa cells were obtained from ATCC (Rockville, MD, USA) (Dong et al. 2014). HepG2 cells were cultured in Eagle's minimum essential medium (DMEM) low glucose with 10% FBS and 10 mg/mL normocin. SK-Hep-1, Huh-7 and HeLa cells were cultured in Eagle's minimum essential medium (DMEM) high glucose with 10% FBS, 50 units/mL penicillin and 50 μg/mL streptomycin.

Cell viability assay

For MTT assay, HepG2 cells were plated and grown to 80–90% confluency and incubated with serum free media for 12 h followed by emodin for 1 h prior to AA treatment for 12 h followed by iron for 2 h (Dong et al. 2014; Choi et al. 2016). For lactate dehydrogenase (LDH) assay, HepG2 cells were plated in 96-well plate and treated as described in MTT assay. LDH assay was performed by CytoTox 96® assay kit (Promega, Madison, WI, USA) as assigned protocols.

Reactive oxygen species (ROS) production

DCFH-DA was used to measure intracellular ROS production in HepG2 cells (Choi et al. 2016). Cells were incubated with 10 μM DCFH-DA for 1 h, and fluorescence was detected by ELISA microplate reader.
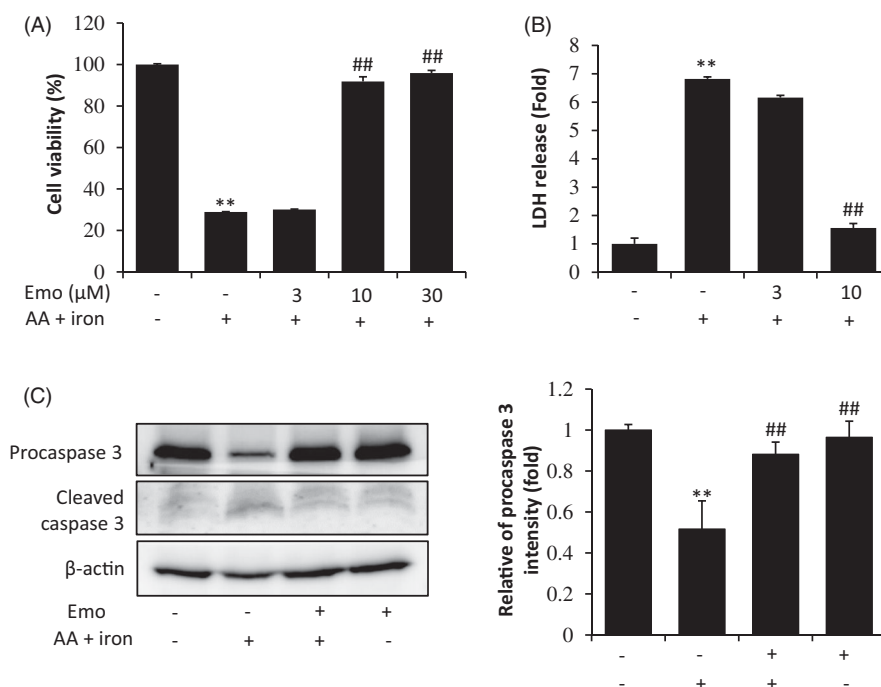
Figure 1. Inhibition of AA + iron induced cell death by emodin. (A) MTT assay and (B) LDH assay. HepG2 cells were incubated with multiple doses (3, 10, 30 μM) of emodin (Emo) 1 h prior to 10 μM AA treatment. After 12 h, cells were incubated with 5 μM iron for 2h. (C) Western blot analysis of apoptosis related proteins was performed with HepG2 cell lysates. HepG2 cells were incubated with AA + iron as describe in panel A with or without 30 μM Emo. All data represent means ± SD of three independent experiments (**$p < 0.01$ between control and AA + iron treated cells; ##$p < 0.01$, #$p < 0.05$ between AA + iron treated cells with or without Emo). AA: arachidonic acid; Emo: emodin.

RNA extraction

Total RNA was individually extracted using Trizol following the manufacturer's instructions (Invitrogen, Carlsbad, CA, USA) (Dong et al. 2014; Choi et al. 2016).

Library preparation and QuantSeq (RNA-seq)

The library was constructed using QuantSeq 3′ mRNA-Seq Library Prep Kit (Lexogen, Inc., Austria) according to the manufacturer's instructions. Samples were prepared with total RNA of 500 ng. Following that an oligo-dT primer containing an Illumina-compatible sequence on its 5′ end was hybridized to the RNA, reverse transcription was performed. The RNA templates were removed, and second strand synthesis was performed by a random primer containing an Illumina-compatible linker sequence on its 5′ end. The double-stranded library was purified using magnetic beads. The library was amplified to add the complete adapter sequences required for cluster generation, and the purification process was done to remove from PCR components. The final library was sequenced using NextSeq 500 (Illumina, Inc., USA) at Ebiogen Inc (Seoul, South Korea) to generate 75pb single-end sequences.

NGS data analysis

QuantSeq 3′ mRNA-Seq reads were aligned using Bowtie2 (Langmead and Salzberg 2012). The alignment files were used to assemble transcripts, to estimate the relative abundances and to detect differential expression of genes. Differentially expressed genes were determined based on the counts from unique and multiple alignments using Bedtools (Quinlan and Hall 2010). The read count data were processed based on Quantile normalization method using EdgeR implemented in R Bioconductor (Gentleman et al. 2004). Gene classification was based on the searches in DAVID (http://david.abcc.ncifcrf.gov/) and Medline databases (http://www.ncbi.nlm.nih.gov/).

Mitochondrial membrane potential (MMP) measurement

HepG2 cells were plated in 6-well plates and treated with emodin, AA and iron as described (Dong et al. 2014; Choi et al. 2016). MMP was measured by FACS Calibur flow cytometer (Becton Dickinson, San Jose, CA. USA).

Immunoblot analysis

Treated cells were lysed in RIPA buffer at 4 °C and lysates were collected. The membrane was developed using ECL (Advensta, Menlo Park, CA, USA) and a gel-doc image analyser (Vilber Lourmat, France) (Dong et al. 2014; Choi et al. 2016).

Animals and treatment

Male C57B/6 mice (5 weeks old, 18 g) were purchased from Charles River Orient Bio (Seongnam, Korea). All in vivo experiment procedures were approved by the Institutional Animal Care and Use Committee of the Daegu Haany University, and were conducted in agreement with the guidelines of the National Institutes of Health. Emodin was dissolved in 40% polyethylene glycol (PEG) and orally injected for three consecutive days (10 and 30 mg/kg) (Ding et al., 2008). After last injection of emodin,

mice were fasted for 16 h and 500 mg/kg APAP was orally injected. All mice were sacrificed 6 h after APAP injection, and blood and liver sample were collected (Ganey et al., 2007). Control group was also treated with 40% PEG.

Haematoxylin and eosin staining

Tissue block was sectioned in 4 µm thick ribbon and applied on slide glass. After deparaffinization in xylene, tissue sections were hydrated in EtOH and stained in haematoxylin for 5 min. After blueing, tissue sections were stained with eosin for 10 sec. Followed by eosin, tissue sections were dehydrated and cleared before mounting.

Statistical analysis

One-way analysis of variance procedures was used to assess significant differences among treatment groups. The criterion for statistical significance was set at $p < 0.05$ or $p < 0.01$.
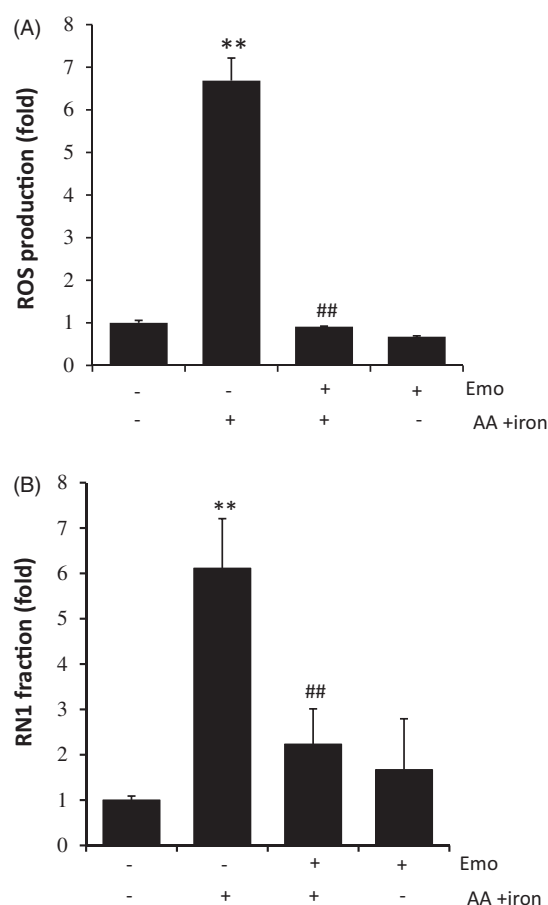

Figure 2. Effect of emodin on AA + iron-induced mitochondrial dysfunction and oxidative stress. (A) Intracellular ROS production measurement by DCF-DA. HepG2 cells were incubated as describe in Figure 1C. (B) Detection of mitochondrial membrane permeability (MMP) change by FACS analysis. RN1 fraction (Low rh123 staining cell population) was expressed as fold change in the graph. All data represent means ± SD of three independent experiments (**$p < 0.01$ between control and AA + iron treated cells; ##$p < 0.01$, #$p < 0.05$ between AA + iron treated cells with or without Emo). AA: arachidonic acid; Emo: emodin; MMP: mitochondrial membrane permeability.

Results

Inhibition of cell death

First, we determined the effects of emodin on cell viability and found that there was no cytotoxicity of emodin in response to concentrations up to 30 μM (data not shown) in HepG2 cells. Next, increasing doses (3, 10, 30 μM) of emodin were applied to investigate the cell protective effect against AA + iron-induced oxidative stress in HepG2 cells. Cell viability was assessed by MTT assay and LDH assay. In the MTT assay, AA + iron treatment decreased cell viability to 28.9% of the control. Emodin treatment of 10 μM and 30 μM attenuated AA + iron induced cytotoxicity (Figure 1(A)). In the LDH assay, AA + iron elevated LDH release up to 6.8-fold compared to control. However, emodin treatment abrogated LDH release induced by these toxicants (Figure 1(B)). In addition, exposure of cells to AA + iron treatment caused cleavage of caspase-3 (Figure 1(C)).

Prevention of ROS production and mitochondrial dysfunction

To investigate the anti-oxidant effects of emodin, we measured intracellular ROS using a spectrophotometer. Although 30 μM emodin alone did not cause intracellular ROS production, the AA + iron-treated group showed 6.68-fold increased ROS compared to the control. However, treatment with emodin completely inhibited elevation of ROS production by AA + iron in HepG2 cells (Figure 2(A)). To examine whether emodin exerts cytoprotective effects via mitochondrial protection, we measured mitochondrial membrane permeability (MMP) by using FACS with Rh123 staining in HepG2 cells. In the AA + iron-treated group, we observed left shift of histogram, which was significantly inhibited by treatment of 30 μM emodin as assessed by FACS analysis (Figure 2(B)). Based on the M1 population, we determined the fold change of the RN1 fraction. The AA + iron treated group showed 6.1-fold more Rh123 positive cells than the control group, and emodin treatment successfully prevented increasing Rh123 positive cells (Figure 2(B)).

LKB1-mediated AMPKα activation

We assessed the effects of emodin in AMPK activation. The useful marker of AMPK activation, phosphorylation of ACC, was observed in HepG2 (Figure 3(A)), SK-Hep-1 (Figure 3(B)) and Huh-7 cells (Figure 3(C)). In HepG2 cells, the maximum activation of AMPKα was observed after 10 min of incubation with 30 μM emodin treatment, while peak values were observed after 30 min for Huh-7 cells and 3 h for SK-Hep-1 cells. To verify whether AMPK activation is mediated by its major upstream target, LKB1, 30 μM emodin was applied to HepG2 cells (Figure 3(D)). We found phosphorylation of LKB1 after 10 mins of emodin incubation for HepG2 cells. Furthermore, there was no activation of AMPKα in HeLa cells, which are LKB1 deficient cells (Figure 3(E)). To confirm a critical role of AMPKα activation in hepatocyte viability, we conducted a MTT assay of HeLa and HepG2 cells. As expected, emodin failed to protect oxidative stress induced cell death (Figure 4(A)). In addition, treatment
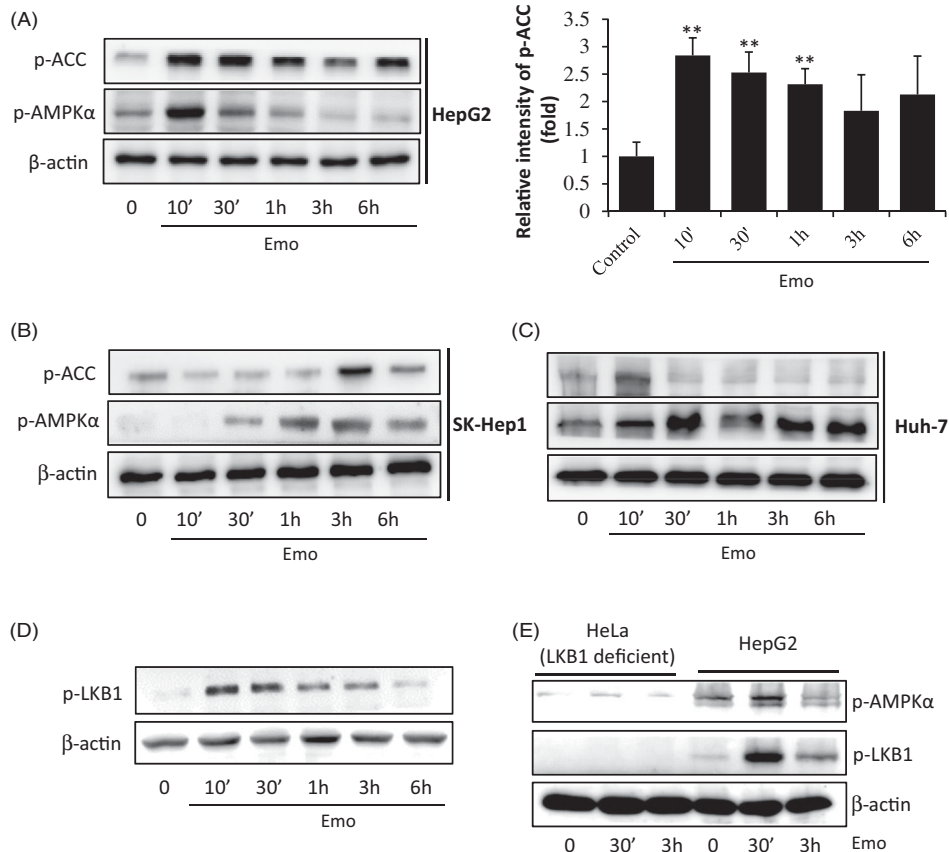

Figure 3. AMPKα activation by emodin. HepG2 cells were incubated in serum free media for 12 h, and then treated with 30 μM Emo for indicated time periods. Western blotting analysis of p-ACC, p-AMPKα and β-actin and band intensity of p-ACC (**$p < 0.01$ between vehicle and Emo-treated cells). Western blotting analysis was performed with HepG2 (A), SK-Hep-1 (B) and Huh-7 cells (C). (D) Expression of p-LKB1 in HepG2 cells. (E) Compare of LKB1-deficient Hela cells and HepG2 cells. Emo: emodin.
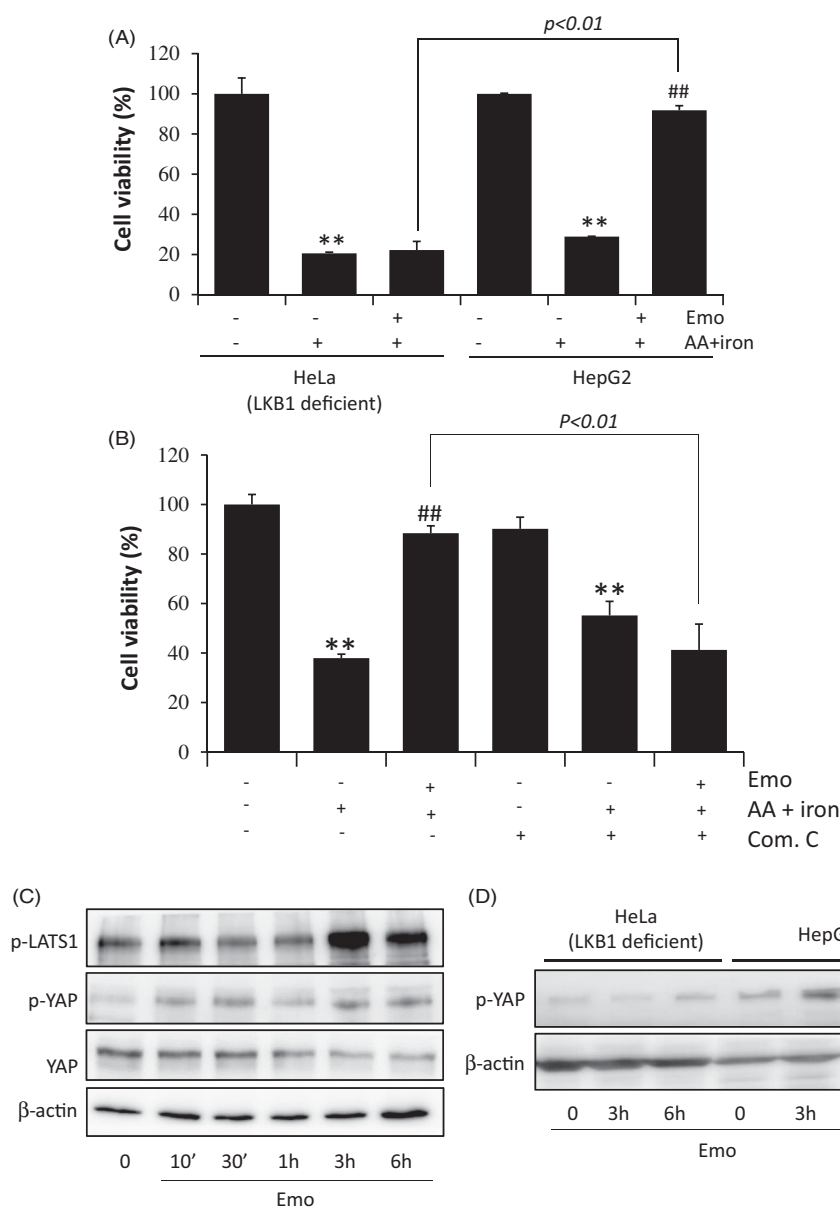
Figure 4. AMPKα and YAP co-relation mediated hepatocyte protective effect of emodin. (A) MTT assay of HeLa and HepG2 cells. HepG2 cells were incubated as describe in Figure 1C. (B) Reversed cell viability by compound C (a chemical inhibitor of AMPK) in HepG2 cells. HeLa cells or HepG2 cells were treated with 10 μM compound C for 30 min and incubated with 10 μM Emo for 1 h, continuously incubated with 10 μM AA for 12 h, and exposed to 5 μM iron for 2 h. All data represent means ± SD of three independent experiments (**$p < 0.01$ between control and AA + iron treated cells; ##$p < 0.01$, #$p < 0.05$ between AA + iron treated cells with or without Emo). (C) Expression of p-LATS1, p-YAP and YAP in HepG2 cells. Hela cells or HepG2 cells were incubated in serum free media for 12 h and treated with 30 μM Emo for indicated time periods. (D) Compare of HeLa cells and HepG2 cells in expression of p-YAP. Com.C: compound C; Emo: emodin.

with compound C (an AMPK inhibitor) significantly prevented the cell protective effect of emodin (Figure 4(B)).

Yap inactivation

Recent findings also showed that the Hippo pathway could be related with oxidative stress (Morinaka et al. 2011; Wada et al. 2011; Xiao et al. 2011). YAP1 is one of the key downstream targets suppressed by the Hippo pathway, and a transcription activator that mediates ROS-triggered signalling. Therefore, we next investigated the effects of emodin in the Hippo signalling pathway related proteins, LATS1 and YAP. In the HepG2 cells, emodin induced the phosphorylation of LATS1 and YAP, and the peak was around 3 h after treatment (Figure 4(C)). Emodin was applied to HeLa cells to verify the relationship of AMPKα and YAP

activation and LKB1 deficient cells showed no change in p-YAP expression in response to emodin stimulation (Figure 4(D)).

Liver protection in mice

AMPK activation by emodin was confirmed *in vivo*. Oral treatments of 10 and 30 mg/kg emodin successfully induced phosphorylation of AMPK and ACC in liver of mice (Figure 5(A)). Next, the oral administration of 10 and 30 mg/kg emodin was assessed to protect the liver. In a mouse model study, APAP was used to induce liver toxicity. The histological analysis revealed that the emodin pre-treated group underwent lower damage of sinusoidal space arrangement and nuclear morphological changes as well as the more arranged patterns of hepatocyte induced by APAP treatment (Figure 5(B)). Oral
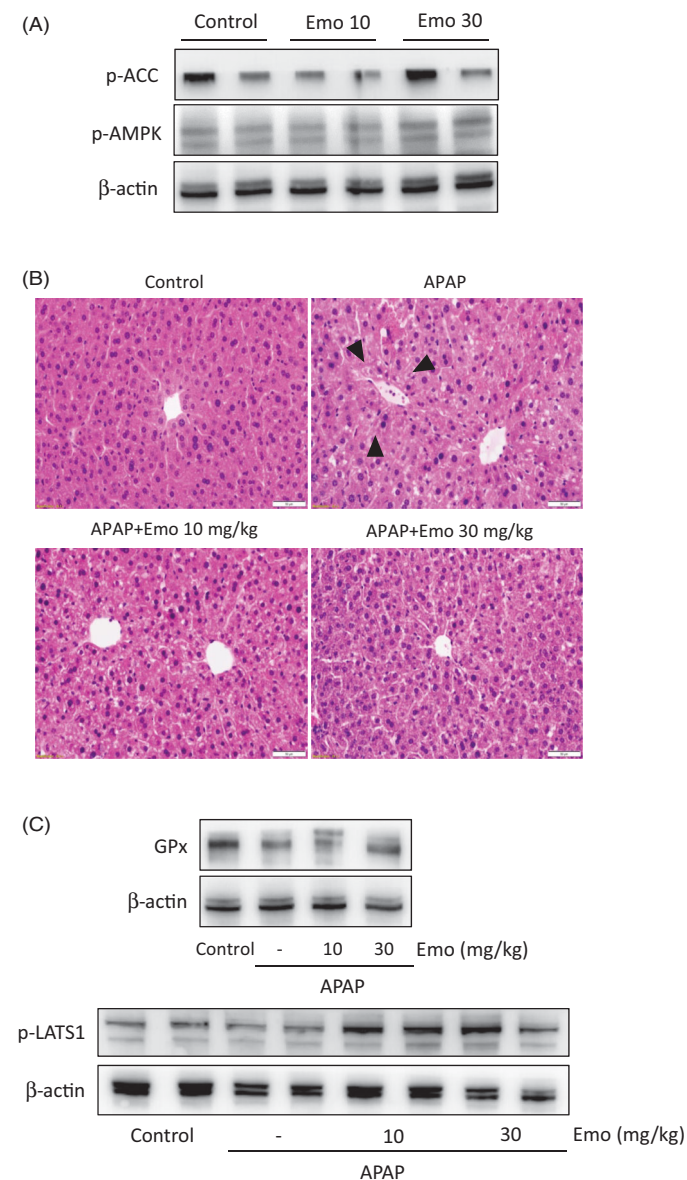
(A)

Table 1. KEGG pathway analysis for differentially expressed genes (DEGs).

KEGG pathway	p Value	DEGs counts
Chemokine signalling pathway	6.5E − 5	14
Cytokine-cytokine receptor interaction	1.9E − 3	13
MAPK signalling pathway	4.5E − 2	10
PI3K-Akt signalling pathway	2.9E − 2	13
TNF signalling pthway	3.1E − 5	11

(B)

(C)

Figure 5. Effect of emodin on acetaminophen (APAP)-induced liver injury in mice. (A) Western blot analysis of p-AMPK and p-ACC. (B) H&E staining. Microscopic images of liver showed hepato-protective effect of Emo against APAP-induced liver damage. APAP-induced serum ALT and AST level was decreased by Emo. Mice were treated with 10 and 30 mg/kg Emo for three consecutive days, followed by 16 h of starvation. Then, mice were orally administrated with 500 mg/kg APAP. (C) Representative immunoblots of glutathione peroxidase (GPx) and p-LATS1. Arrows indicate degeneration of hepatocytes. Bar = 50 μm. APAP: acetaminophen; Emo: emodin; GPx: glutathione peroxidase.

administration of emodin also decreased the APAP-induced ALT and AST levels, which are biological markers of liver tissue damage (data not shown). Moreover, the immunoblot assessments revealed that emodin markedly recovered the dysregulation of antioxidant enzyme (i.e., glutathione peroxidase) and its related signalling induced by APAP (Figure 5(C)).

Differentially expressed genes (DEGs) in RNA-seq analysis data

We conducted quantitative RNA-seq analysis using RNA samples from control and 10 mg/kg emodin treated mice liver tissues and attempted to compare gene expression profiles between them to

identify target genes and related pathways that might be responsible for the regulation of these genes. Genes differentially regulated by more than 10-fold in the emodin injected group compared to the control group were found and listed in Supplementary Table 1. Comparison of the gene expression profiles identified 416 genes for which expression levels (fold change > 2 and p-value < 0.05) were changed after emodin treatment. These genes were likely involved in the KEGG pathway (61 genes), chemokine signalling pathway (14 genes), cytokine-cytokine receptor interaction (13 genes), MAPK signalling pathway (10 genes), PI3K-Akt signalling pathway (13 genes) and TNF signalling pathway (11 genes; Table 1).

Several of the most strongly induced genes were targets of the AMPK signalling pathway and the Hippo pathway (Figure 6(A); Tables 2 and 3). Prkaa1 (5′-AMP-activated protein kinase catalytic subunit α-1) was significantly upregulated (1.25-fold), while Prkaa2 (5′-AMP-activated protein kinase catalytic subunit α-2) and Prkab1 (5′-AMP-activated protein kinase subunit β-1) were significantly downregulated (0.08-fold: Prkaa2, 0.78-fold: Prkab1) in response to emodin when compared with the control (Figure 6(A); Table 2). The commonly known YAP target genes, Lats1 (Large Tumour Suppressor Kinase 1) and Mob1b (MOB Kinase Activator 1B), showed a striking level of upregulation (1.15-fold: Lats1, 1.36-fold: Mob1b; Figure 6(B); Table 2). However, Ajuba, a negative regulator of the Hippo signalling pathway, was greatly downregulated in response to emodin injection (0.29-fold; Figure 6(B); Table 2). qPCR also confirmed the effect of emodin on the gene expressions. In addition, emodin increased the protein expression of p-AMPKα and p-YAP in the livers of mice as assessed by immunoblot analysis (data not shown). Thus, these data show that emodin triggers the induction of AMPK and Hippo signalling pathways.

Discussion

Oxidative stress causes cellular damage, aging and apoptosis and activates pro-inflammatory factors that induce inflammation (Varga et al. 2015). Normally, ROS is generated during oxygen metabolism (Gupta et al. 2014). In addition, ROS is considered as carcinogen because of its effects on mutagenesis, tumour promotion and progression (Waris and Ahsan 2006). Therefore, the regulation of oxidative stress in tissue is an important strategy to prevent a line of disease. Here, we found that emodin had the ability to inhibit oxidative stress in hepatocytes stimulated with AA + iron as well as in mice injected with APAP. Moreover, we suggested the AMPK pathway as a mechanism of the effects of emodin.

Although acute pharmacological activation of AMPK was shown to decrease glutathione and facilitate oxidative stress, AMPK has been found to have beneficial functions in the cells including anti-oxidant, anti-tumour and anti-inflammation activities (Kim et al. 2009; Shin and Kim 2009). Oxidative stress
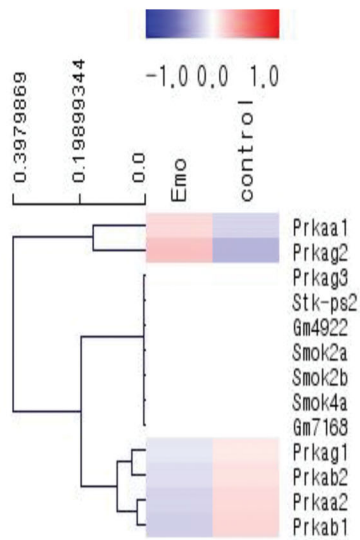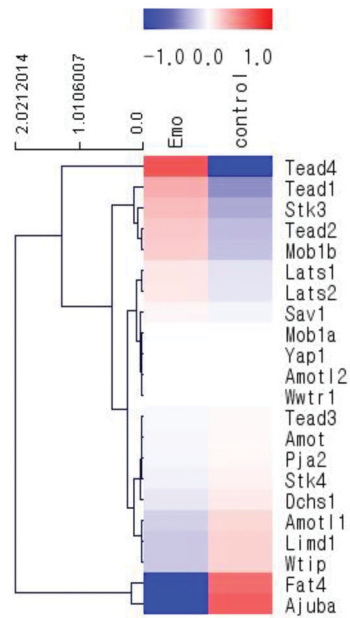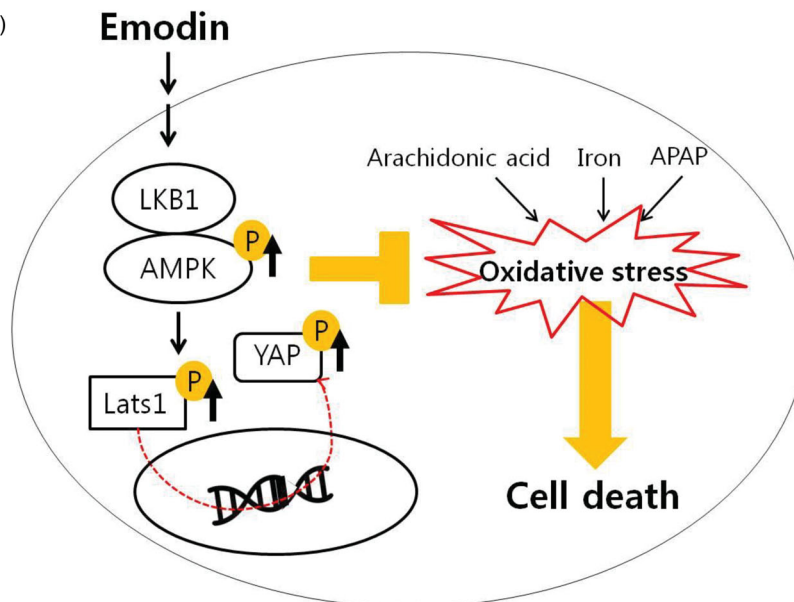
Figure 6. Activation of AMPK and YAP pathway by emodin in mouse liver. The heatmap depicts the changes in AMPK signalling pathway (A) and Hippo pathway signalling (B) related gene expression between control group and 10 mg/kg Emo-treated group using QuantSeq 3′ mRNA-Seq data. Red indicates higher gene expression values and blue indicates lower gene expression values. (C) Scheme of the mechanism. Emo: emodin.

causes binding of the mitochondrial protein to reactive metabolites, leading to mitochondrial dysfunction (McGill et al. 2012). In our previous studies, some novel AMPK activators (e.g., isoliquiritigenin, isorhamnetin and sauchinone) were reported to attenuate AA and iron-induced oxidative stress via AMPK mediated signalling pathways (Kim et al. 2009; Shin and Kim 2009; Dong et al. 2014).

Upon energy stress, the activation loop of α-subunit is exposed by conformational change, allowing it to be activated by phosphorylation of its upstream kinase, LKB1 (Choi et al. 2010). Activated AMPK phosphorylates various target proteins (Shaw et al. 2005). Though these signalling pathways, AMPK could

protect mitochondria against oxidative damage (Wu and Wei 2012). In this study, emodin significantly induced activation of AMPK and LKB1. Moreover, it had no protective effect under AMPK inhibition by compound C and LKB1 deficiency in Hela cells.

It has been reported that YAP1 protects cardiomyocytes against ROS-induced cell death and the reduced expression of YAP1 indicates the weak defence mechanism against oxidative stress (Del Re et al. 2013, Pan 2010; Wu et al. 2013; Shao et al. 2014). Based on these reports, we investigated the effects of emodin on the Hippo pathway. Emodin markedly upregulated phosphorylation of YAP and LATS1. Considering this compound

Table 2. Regulated genes related to AMPK pathway emodin injected group compared to control group.

Gene symbol		Full name	Fold change	Description
Up-regulated genes	Prkaa1	5′-AMP-activated protein kinase catalytic subunit alpha-1	1.246	A regulator of cellular polarity by remodelling the actin cytoskeleton
	Prkag2	protein kinase, cGMP-dependent, type II	1.008	A heterotrimeric protein composing AMP-activated protein kinase
Down-regulated genes	Prkaa2	5′-AMP-activated protein kinase catalytic subunit alpha-2	0.0803	A catalytic subunit of the AMP-activated protein kinase
	Prkab1	5′-AMP-activated protein kinase subunit beta-1	0.783	A non-catalytic subunit of the AMP-activated protein kinase

Table 3. Regulated genes related to Hippo signalling pathway emodin injected group compared to control group.

Gene symbol		Full name	Fold change	Description
Up-regulated genes	Tead4	TEA Domain Transcription Factor 4	4.047	Transcription factor which plays a key role in the Hippo signalling pathway
	Tead1	TEA Domain Transcription Factor 1	1.677	Paralog of TEAD 4
	Stk3	Serine/Threonine Kinase 3	1.509	Repress proliferation of mature hepatocytes
	Mob1b	MOB Kinase Activator 1B	1.356	Binding with LATS1 and phosphorylates and inactivates YAP1
	Lats1	Large Tumour Suppressor Kinase 1	1.151	Inhibiting translocation into the nucleus of YAP1 by phosphorylation
Down-regulated genes	Amotl1	Angiomotin Like 1	0.790	Encoding peripheral membrane protein that is a component of tight junctions
	Limd1	LIM Domains Containing 1	0.761	Involved in several cellular processes such as repression of gene transcription, cell differentiation and proliferation
	Wtip	WT1 Interacting Protein	0.760	Involved transcription corepressor activity
	Fat4	FAT Atypical Cadherin 4	0.340	Plays a role in inhibition of YAP1-mediated neuroprogenitor cell proliferation and differentiation
	Ajuba	Ajuba LIM Protein	0.287	Negatively regulates the Hippo signalling pathway and antagonises phosphorylation of YAP1

does not increase the phosphorylation of YAP in LKB1 deficient Hela cells, YAP inactivation by emodin might be related to the AMPK pathway.

We also performed quantitative RNA-seq analysis. With the advent and continuous refinement of NGS technology, total RNA-sequencing (RNA-seq) may be the most promising solution to identify changes in transcriptional machinery. However, this can likely be deleted (Wang et al. 2009). In addition, RNA-seq has completely replaced microarray tools because it can accurately profile complete transcriptomes at cheaper rate and can be performed without exact knowledge of the genomic sequence in a species (Marioni et al. 2008). To identify the target genes and the related pathways that might be responsible for the effects of emodin treatment, we conducted quantitative RNA-seq analysis of RNA samples extracted from both control and emodin treated mice liver tissues and found that strongly induced genes were related to the AMPK and the Hippo pathway.

APAP is an analgesic drug that is used worldwide. Treatment with APAP results in production of NAPQI, which is a well-known reactive metabolite of APAP, by liver cytochrome P450s (CYPs). Overdose of APAP lead to production of excessive amounts of NAPQI, which can cause hepatic GSH depletion and reduced redox capacity. These conditions can result in the accumulation oxidative stress in liver tissue (Truong et al. 2016). Therefore, APAP is often used as a liver toxicity inducer in anti-oxidant and hepato-protective drug screening animal models (Lin et al. 2001; Chen et al. 2009; Olaleye et al. 2010). In the present study, emodin successfully inhibited the elevation of plasma markers of hepatotoxicity and oxidative tissue damage in the liver induced by APAP. Because APAP also promotes extrahepatic damage, it is needed to determine to provide a more

detailed analysis of the potential protective actions of emodin in the future.

Collectively, emodin attenuated oxidative damage in the hepatocyte cell line and in mice. In cells, emodin inhibited ROS generation and mitochondria damage induced by AA + iron was mediated via LKB1-AMPK and Hippo-YAP1 signals, which were also confirmed by NGS. In mice, emodin successfully decreased APAP-induced oxidative damage in the liver. Taken together, the results of this study suggest that emodin could be a potential hepatoprotectant as well as an antioxidant.

Disclosure statement

The authors declare that there are no conflicts of interest.

ORCID

Young Woo Kim 🆔 http://orcid.org/0000-0002-3323-7106

References

Caro AA, Cederbaum AI. 2001. Synergistic toxicity of iron and arachidonic acid in HepG2 cells overexpressing CYP2E1. Mol Pharmacol. 60(4):742–752.

Chen YH, Lin FY, Liu PL, Huang YT, Chiu JH, Chang YC, Man KM, Hong CY, Ho YY, Lai MT. 2009. Antioxidative and hepatoprotective effects of magnolol on acetaminophen-induced liver damage in rats. Arch Pharm Res. 32(2):221–228.

Chen YC, Shen SC, Lee WR, Hsu FL, Lin HY, Ko CH, Tseng SW. 2002. Emodin induces apoptosis in human promyeloleukemic HL-60 cells accompanied by activation of caspase 3 cascade but independent of reactive oxygen species production. Biochem Pharmacol. 64(12):1713–1724.

Choi SH, Kim YW, Kim SG. 2010. AMPK-mediated GSK3β inhibition by isoliquiritigenin contributes to protecting mitochondria against iron-catalyzed oxidative stress. Biochem Pharmacol. 79(9):1352–1362.

Choi HY, Lee JH, Jegal KH, Cho IJ, Kim YW, Kim SC. 2016. Oxyresveratrol abrogates oxidative stress by activating ERK–Nrf2 pathway in the liver. Chem Biol Int. 245:110–121.

Del Re DP, Yang Y, Nakano N, Cho J, Zhai P, Yamamoto T, Zhang N, Yabuta N, Nojima H, Pan D, et al. 2013. Yes-associated protein isoform 1 (Yap1) promotes cardiomyocyte survival and growth to protect against myocardial ischemic injury. J Biol Chem. 288(6):3977–3988.

Ding Y, Zhao L, Mei H, Zhang SL, Huang ZH, Duan YY, Ye P. 2008. Exploration of emodin to treat alpha-naphthylisothiocyanate-induced cholestatic hepatitis via anti-inflammatory pathway. Eur J Pharmacol. 590(1–3):377–386.

Dong GZ, Lee JH, Ki SH, Yang JH, Cho IJ, Kang SH, Zhao RJ, Kim SC, Kim YW. 2014. AMPK activation by isorhamnetin protects hepatocytes against oxidative stress and mitochondrial dysfunction. Eur J Pharmacol. 740:634–640.

Emerling BM, Weinberg F, Snyder C, Burgess Z, Mutlu GM, Viollet B, Budinger GS, Chandel NS. 2009. Hypoxic activation of AMPK is dependent on mitochondrial ROS but independent of an increase in AMP/ATP ratio. Free Radic Biol Med. 46(10):1386–1391.

Ganey PE, Luyendyk JP, Newport SW, Eagle TM, Maddox JF, Mackman N, Roth RA. 2007. Role of the coagulation system in acetaminophen-induced hepatotoxicity in mice. Hepatology. 46(4):1177–1186.

Gentleman RC, Carey VJ, Bates DM, Bolstad B, Dettling M, Dudoit S, Ellis B, Gautier L, Ge Y, Gentry J, et al. 2004. Bioconductor: open software development for computational biology and bioinformatics. Genome Biol. 5(10):R80.

Gijón MA, Spencer DM, Siddiqi AR, Bonventre JV, Leslie CC. 2000. Cytosolic phospholipase A2 is required for macrophage arachidonic acid release by agonists that Do and Do not mobilize calcium. Novel role of mitogen-activated protein kinase pathways in cytosolic phospholipase A2 regulation. J Biol Chem. 275(26):20146–20156.

Gupta RK, Patel AK, Shah N, Choudhary AK, Jha UK, Yadav UC, Gupta PK, Pakuwal U. 2014. Oxidative stress and antioxidants in disease and cancer. Asian Pac Cancer Prev. 15(11):4405–4409.

Horie T, Ono K, Nagao K, Nishi H, Kinoshita M, Kawamura T, Wada H, Shimatsu A, Kita T, Hasegawa K. 2008. Oxidative stress induces GLUT4 translocation by activation of PI3-K/Akt and dual AMPK kinase in cardiac myocytes. J Cell Physiol. 215(3):733–742.

Kim YW, Lee SM, Shin SM, Hwang SJ, Brooks JS, Kang HE, Lee MG, Kim SC, Kim SG. 2009. Efficacy of sauchinone as a novel AMPK-activating lignan for preventing iron-induced oxidative stress and liver injury. Free Radic Biol Med. 47(7):1082–1092.

Langmead B, Salzberg SL. 2012. Fast gapped-read alignment with Bowtie 2. Nat Methods. 9(4):357–359.

Lee JH, Kim JM, Kim C. 2003. Pharmacokinetic analysis of rhein in Rheum undulatum L. J Ethnopharmacol. 84(1):5–9.

Li S, Tan HY, Wang N, Zhang ZJ, Lao L, Wong CW, Feng Y. 2015. The role of oxidative stress and antioxidants in liver diseases. Int J Mol Sci. 16(11):26087–26124.

Lin CC, Hsu YF, Lin TC, Hsu HY. 2001. Antioxidant and hepatoprotective effects of punicalagin and punicalin on acetaminophen-induced liver damage in rats. Phytother Res. 15(3):206–212.

Marioni JC, Mason CE, Mane SM, Stephens M, Gilad Y. 2008. RNA-seq: an assessment of technical reproducibility and comparison with gene expression arrays. Genome Res. 18(9):1509–1517.

Matsuda H, Tomohiro N, Hiraba K, Harima S, Ko S, Matsuo K, Yoshikawa M, Kubo M. 2001. Study on anti-Oketsu activity of rhubarb II. Anti-allergic effects of stilbene components from Rhei undulati Rhizoma (dried rhizome of Rheum undulatum cultivated in Korea). Biol Pharm Bull. 24(3):264–267.

McGill MR, Williams CD, Xie Y, Ramachandran A, Jaeschke H. 2012. Acetaminophen-induced liver injury in rats and mice: comparison of protein adducts, mitochondrial dysfunction, and oxidative stress in the mechanism of toxicity. Toxicol Appl Pharmacol. 264(3):387–394.

Morinaka A, Funato Y, Uesugi K, Miki H. 2011. Oligomeric peroxiredoxin-I is an essential intermediate for p53 to activate MST1 kinase and apoptosis. Oncogene. 30(40):4208–4218.

Olaleye MT, Akinmoladun AC, Ogunboye AA, Akindahunsi AA. 2010. Antioxidant activity and hepatoprotective property of leaf extracts of Boerhaavia diffusa Linn against acetaminophen-induced liver damage in rats. Food Chem Toxicol. 48(8–9):2200–2205.

Pan D. 2010. The Hippo signaling pathway in development and cancer. Dev Cell. 19(4):491–505.

Pang X, Liu J, Li Y, Zhao J, Zhang X. 2015. Emodin inhibits homocysteine-induced C-reactive protein generation in vascular smooth muscle cells by regulating PPARγ expression and ROS-ERK1/2/p38 signal pathway. PLoS One. 10(7):e0131295.

Purohit V, Brenner DA. 2006. Mechanisms of alcohol-induced hepatic fibrosis: a summary of the Ron Thurman Symposium. Hepatology. 43(4):872–878.

Quinlan AR, Hall IM. 2010. BEDTools: a flexible suite of utilities for comparing genomic features. Bioinformatics. 26(6):841–842.

Shao D, Zhai P, Del Re DP, Sciarretta S, Yabuta N, Nojima H, Lim DS, Pan D, Sadoshima J. 2014. A functional interaction between Hippo-YAP signaling and FoxO1 mediates the oxidative stress response. Nat Commun. 5(1):3315.

Shaw RJ, Lamia KA, Vasquez D, Koo SH, Bardeesy N, DePinho RA, Montminy M, Cantley LC. 2005. The kinase LKB1 mediates glucose homeostasis in liver and therapeutic effects of metformin. Science. 310(5754):1642–1646.

Shin SM, Kim SG. 2009. Inhibition of arachidonic acid and iron-induced mitochondrial dysfunction and apoptosis by oltipraz and novel 1, 2-dithiole-3-thione congeners. Mol Pharmacol. 75(1):242–253.

Truong VL, Ko SY, Jun M, Jeong WS. 2016. Quercitrin from Toona sinensis (Juss.) M. Roem. attenuates acetaminophen-induced acute liver toxicity in HepG2 Cells and mice through induction of antioxidant machinery and inhibition of Inflammation. Nutrients. 8(7):431.

Varga ZV, Giricz Z, Liaudet L, Haskó G, Ferdinandy P, Pacher P. 2015. Interplay of oxidative, nitrosative/nitrative stress, inflammation, cell death and autophagy in diabetic cardiomyopathy. Biochim Biophys Acta. 1852(2):232–242.

Wada KI, Itoga K, Okano T, Yonemura S, Sasaki H. 2011. Hippo pathway regulation by cell morphology and stress fibers. Development. 138(18):3907–3914.

Wang Z, Gerstein M, Snyder M. 2009. RNA-Seq: a revolutionary tool for transcriptomics. Nat Rev Genet. 10(1):57–63.

Waris G, Ahsan H. 2006. Reactive oxygen species: role in the development of cancer and various chronic conditions. J Carcinog. 5(1):14.

Wu SB, Wei YH. 2012. AMPK-mediated increase of glycolysis as an adaptive response to oxidative stress in human cells: implication of the cell survival in mitochondrial diseases. Biochim Biophys Acta. 1822(2):233–247.

Wu H, Xiao Y, Zhang S, Ji S, Wei L, Fan F, Geng J, Tian J, Sun X, Qin F, et al. 2013. The Ets transcription factor GABP is a component of the Hippo pathway essential for growth and antioxidant defense. Cell Rep. 3(5):1663–1677.

Xiao L, Chen D, Hu P, Wu J, Liu W, Zhao Y, Cao M, Fang Y, Bi W, Zheng Z, et al. 2011. The c-Abl-MST1 signaling pathway mediates oxidative stress-induced neuronal cell death. J Neurosci. 31(26):9611–9619.

Xue J, Ding W, Liu Y. 2010. Anti-diabetic effects of emodin involved in the activation of PPARγ on high-fat diet-fed and low dose of streptozotocin-induced diabetic mice. Fitoterapia. 81(3):173–177.

Yoo MY, Oh KS, Lee JW, Seo HW, Yon GH, Kwon DY, Kim YS, Ryu SY, Lee BH. 2007. Vasorelaxant effect of stilbenes from rhizome extract of rhubarb (Rheum undulatum) on the contractility of rat aorta. Phytother Res. 21(2):186–189.